NUCLEAR PHYSICS

The São Paulo Potential and the 3He Breakup Reaction at 130 MeV on 93Nb and 197Au

E. V. Chimanski[1] · L. A. Souza[2] · B. V. Carlson[2]

Abstract

Nuclear reactions induced by weakly bound nuclei often result in the emission of light particles as products of the projectile breakup. The incident particle is expected to fragment before reaching the interior of the target nuclei, a characteristic that tends to favor forward angular emission. Although the first models developed for such reactions were proposed many decades ago by Udagawa and Tamura, Ichimura, Austern, Vincent, and Kasano, and Hussein and McVoy, to this date most of the attention has been dedicated to the breakup of the deuteron and other very weakly bound systems, while more strongly bound projectiles have not been fully explored. Here, we describe the production of protons and deuterons from the breakup of 3He. The breakup of 3He on two heavy targets, 93Nb and 197Au, is analyzed in this study. However, the incoming energy involved is much larger than that of the standard phenomenological optical potentials available in the literature for the 3He entrance channel. We have overcome this difficulty by using the São Paulo potential and adjusting the nuclear diffusivity. The deuteron inclusive spectra were calculated at several angles and compared well with the experimental data. Theoretical proton emission predictions are also given for future reference, since no inclusive measurements were performed for the targets under study. One of our goals is to verify the description of deuteron emission from fast projectiles, for which many partial waves contribute to the scattering process.

Keywords Breakup · SP potential · Inclusive emissions · Nuclear reactions

1 Introduction

Nuclear reactions induced by composite particles, such as deuterons, He, Be, and Li nuclei, play a key role in accessing the structural properties of these projectiles, as well as serving as a direct method of generating light particle beams. The study of projectile breakup has garnered strong attention from the nuclear physics community for several decades now. Breakup of the deuteron into proton and neutron has been extensively investigated due to the simplicity of the projectile and its fragments as well as a variety of possible applications, from radioisotope production [1, 2] to modern surrogate reactions strategies

[3]. The study of weakly bound projectiles, the so-called halo nuclei, has motivated upgrades in many laboratories, which now provide a great variety of experimental data on such reactions [4, 5]

Many possible outgoing channels can be open in a reaction involving a composite projectile. At intermediate and higher energies, the direct reaction mechanism dominates the reaction dynamics and one can associate much of the particle emission with fast events. The slow process of projectile absorption, compound nucleus formation, and particle evaporation becomes less significant at higher energy, although these reactions are still present and play an important role in emission at backward angles.

Most studies on ³He-induced breakup reactions were conducted in the 1980s, when more refined theoretical models of these reactions were being developed. Although there is great interest at present in this type of reaction, the relatively strong binding and simple structure of ³He have contributed to a general lack of interest in its breakup. Little attention has been given to the excellent experimental data provided by Matsuoka et al. [6], Djaloeis et al. [7], and Aarts et al. [8]. The breakup of ³He into protons and deuterons has

✉ E. V. Chimanski
  chimanski1@llnl.gov

1   Lawrence Livermore National Laboratory 7000 East Avenue, Livermore, CA 94550, USA

2   Departamento de Física, Instituto Tecnológico de Aeronáutica, DCTA, 12228-900, São José dos Campos, SP, Brazil

thus not been fully explored within a more modern reaction formalism.

In this work, we analyze part of the experimental data provided by Djaloeis et al. [7] by comparing these with calculations of the proton and deuteron inclusive emission spectra and double differential cross sections for reactions induced by ^{3}He at 130 MeV on two heavy targets, ^{93}Nb and ^{197}Au. We use the post-form DWBA framework to calculate elastic and nonelastic breakup cross sections assuming a zero-range interaction between the two fragments. One of our objectives is to determine a good optical potential for the entrance channel, which we hope to extend to a global characterization of inclusive emissions from ^{3}He-induced reactions on different target nuclei.

We have organized this work as follows: we provide a brief overview of the reaction formalism employed in the Section 2. Sections 3 and 4 compare our calculations to the experimental data and give our concluding remarks, respectively.

2 Theoretical Formalism and Optical Potentials

The theoretical study of projectile breakup had its origins in the 1940s with the well-known work of Serber on deuteron breakup [9]. In the 1980s, the breakup models were extended by several groups, using the DWBA to describe nonelastic breakup, also called incomplete fusion [10–15]. For the sake of brevity, we will only sketch a basic outline of the inclusive breakup reaction formalism. For a more detailed discussion on the development of the modern models, we point out the following recent references [4, 16–19].

The energy and angular distributions of a breakup reaction characterize it as a direct process. The inclusive particle emission cross sections consist of two principal components, an elastic (EB) one and a nonelastic breakup (NEB) one. Taking the reaction to be ^{3}He $+ A \rightarrow b + X$, and using the zero-range post-form DWBA, we can write the double differential inclusive cross section as

$$\frac{d^3\sigma}{dk_b^3} = \frac{d^3\sigma^{\text{EB}}}{dk_b^3} + \frac{d^3\sigma^{\text{NEB}}}{dk_b^3}, \tag{1}$$

where b represents one of the projectile fragments ($b = p$ or $b = d$).

If we represent the projectile with the label a, the nonelastic contribution is obtained by calculating the reaction cross section of $x + A$, using the imaginary part of the $x + A$ optical potential,

$$\frac{d^3\sigma^{\text{NEB}}}{dk_b^3} = -\frac{2(2\pi)^{-3}}{\hbar v_a} \langle \Psi_x | W_{xA} | \Psi_x \rangle, \tag{2}$$

and the effective wave function for the particle x after breakup,

$$|\Psi_x\rangle = D_0 \left(\chi_b^{(-)} G_x^{(+)} \Lambda | \chi_a^{(+)} \right), \tag{3}$$

which we calculate in the zero-range approximation

$$V_a(\vec{r})\phi_a(\vec{r}) \approx D_0 \delta(\vec{r}) \tag{4}$$

with $D_0 = -128.75$ MeV fm$^{3/2}$.

The elastic breakup contribution is obtained by integrating the elastic breakup differential cross section over the energy and angle of the other fragment:

$$\frac{d^3\sigma^{\text{EB}}}{dk_b^3} = \frac{(2\pi)^{-5}}{\hbar v_a} \int dk_x^3 |\langle b, x|T|a\rangle|^2 \times \delta(E_a + \epsilon - E_x - E_b). \tag{5}$$

where ϵ is the separation energy of the projectile into b and x. We approximate the elastic breakup transition amplitude by its DWBA:

$$\langle b, x|T|a\rangle = \langle \chi_b^{(-)} \chi_x^{(-)} | V_a | \chi_a^{(+)} \phi_a \rangle \tag{6}$$

and simplify this further using the zero-range approximation, to write

$$\langle b, x|T|a\rangle = D_0 \langle \chi_b^{(-)} \chi_x^{(-)} \Lambda | \chi_a^{(+)} \rangle, \tag{7}$$

where Λ accounts for finite-range effect corrections [20].

This approach has already been used with a fair degree of success to describe experimental data for the case of reactions induced by deuterons ($a = d$). Inclusive proton emission cross sections were obtained for different targets and energies and compared to experimental data in [4, 16, 17, 19].

Here, we obtain the proton and deuteron distorted waves by employing the Koning-Delaroche [21] and Han-Shi-Shen [22] optical potentials, respectively. For the ^{3}He-target interaction, we first attempted to use the standard Becchetti-Greenlees [23] optical potential, but without success, due to the high energy of the projectile. The folding-like São Paulo (SP) potential [24, 25] was then employed in the incident channel both nuclei. For the sake of simplicity in its implementation, we performed a best fit of a Wood-Saxon-like function to the São Paulo potential. This provided potential parameters that could be easily used in the breakup calculation.

In Fig. 1, we show the real part of the SP potential, for the ^{3}He $+ ^{197}$Au interaction, in comparison to the best Wood-Saxon fit. Although the shape and strength of the SP potential are well described by a Wood-Saxon function, we found it to have a very large diffusivity $a_{\text{SP}} \approx 0.95$ fm, for both ^{93}Nb and ^{197}Au. This leads to a too absorptive imaginary potential, when we use the standard prescription of $W(r) = N_I V(r)$. We have thus fixed the diffusivity to a more standard value of $a_0 = 0.65$ fm and maintained it fixed throughout the calculations. We still take the strength
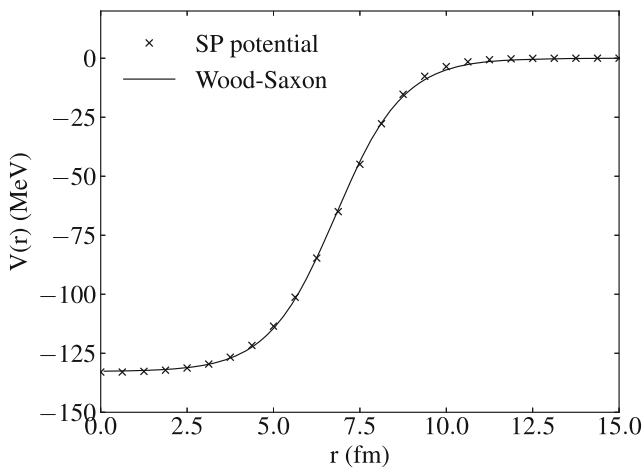
Fig. 1 Real part of the São Paulo optical potential for the entrance channel ^{3}He-^{197}Au (markers). The best fit of a Wood-Saxon-like function is also shown (solid line). The adjusted parameters are explained in the text and given in Table 1
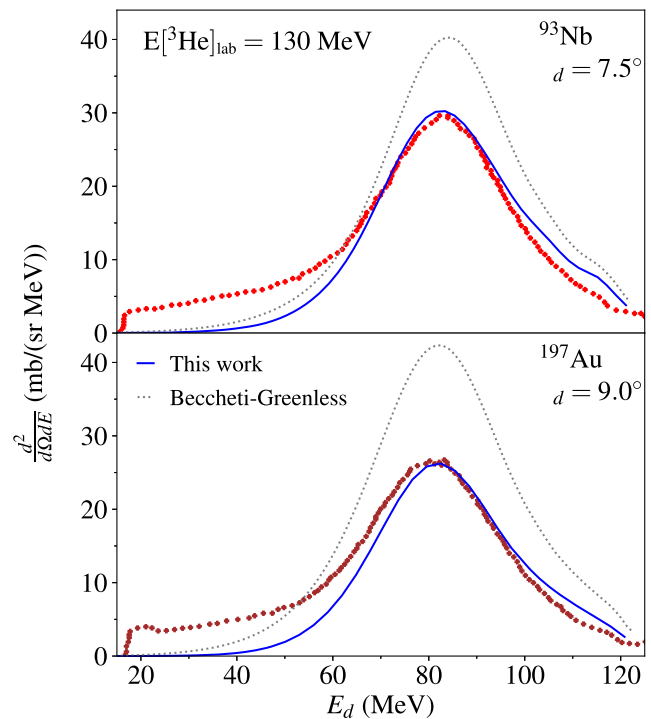

Fig. 2 Inclusive differential deuteron spectra at $\theta_d = 7.5°$ for ^{93}Nb (top) and $\theta_d = 9.0°$ for ^{197}Au (bottom) targets at 130 MeV of incident energy. Spectra obtained with the Beccheti-Greenlees optical potential and the modified São Paulo potential for the ^{3}He-target potential are compared (see Table 1 for parameters). The experimental data are taken from [7]

V_0 and the reduced radius r_0 ($R = r_0 A^{1/3}$) parameters from the fit to the SP potential and take the imaginary part of the interaction to be $W_0 = 0.78\, V_0$, as is usually done with the SP potential. The parameters used for the two targets are given in Table 1. The same geometrical parameters are employed for both the real and imaginary parts of the potentials.

3 Inclusive Cross Sections

Although we have restricted this study to reactions on heavy targets, we have converted the differential cross sections to the laboratory (LAB) frame for comparison to the experimental measurements. Differences of a few percent between the calculated CM and LAB cross sections can be observed. All quantities shown are in the LAB frame, unless said otherwise. The experimental data for deuteron emissions were extracted from Djaloeis et al. [7] and an ^{3}He separation energy of $\epsilon = -5.49$ MeV was employed.

In Fig. 2, we present the deuteron differential spectrum at the fixed angle of $\theta_d = 7.5°$ for ^{93}Nb and at $\theta_d = 9.0°$ for ^{197}Au. The Beccheti-Greenlees potential reaches its limit of application at energies of about 40 MeV [7, 26] and cannot be reliably used to model faster incident projectiles.

Table 1 Reduced radius and potential depth of the Wood-Saxon potential adjusted to the São Paulo potential for the ^{3}He-induced reactions on ^{93}Nb and ^{197}Au at 130 MeV

Target	r_0 (fm)	V (MeV)	W (MeV)	a (fm)
^{93}Nb	1.126	−131.95	−102.90	0.65
^{197}Au	1.169	−132.74	−103.54	0.65

We have found that the SP potential, on the other hand, provides excellent agreement with the experimental data. The center of the distribution around ~ 80 MeV is well reproduced, especially for ^{93}Nb. Small shifts associated with details of the geometry of the nucleus can be seen in the calculations. The low-energy part of the spectra is expected to have contributions from compound nucleus evaporation, a component not calculated in our model. With the success of this first comparison, we have extended our calculations of deuteron emissions to different angles.

In Fig. 3, we show deuteron differential spectra at several angles. One observes again a very good correspondence between our calculations and the experimental data. The lower energy part of the experimental spectra, corresponding to compound nucleus emission, becomes more prominent as the scattering angle increases. According to our calculations, the direct breakup component contributes to the deuteron emission at energies higher than about 40 MeV for both ^{93}Nb and ^{197}Au nuclei. At $\theta_d = 21°$, the compound emission dominates the reaction. Our calculations tend to overestimate the cross sections for the higher energy part of the spectra, a characteristic that is associated with the geometry and diffuseness of the optical potential. The description of these shifts will be addressed in a future work.
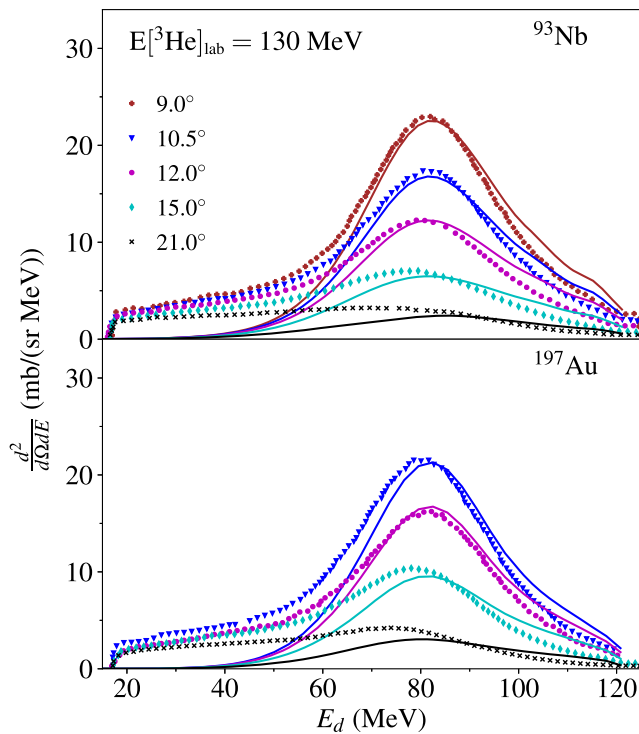
Fig. 3 Inclusive deuteron spectra from the breakup of ^{3}He on ^{93}Nb (top) and ^{197}Au (bottom) targets for several angles. Optical potential parameters in the entrance channel are given in Table 1. The experimental data are taken from [7]

Fig. 4 Inclusive proton spectra from the breakup of ^{3}He on ^{93}Nb (top) and ^{197}Au (bottom) targets for several angles

Before closing, we present in Fig. 4 the differential spectra of protons for several fixed scattering angles. Although we have no experimental data with which to compare, the calculations serve as a future reference and provide a more complete description of the inclusive breakup emission from ^{3}He. The distributions are centered around $\approx$ 45 MeV, and the strength of the cross section decreases for larger scattering angles, as in the case of deuterons. One would expect a somewhat larger contribution from compound nucleus emission here, as is usually the case.

4 Concluding Remarks

In this paper, we have studied the inclusive differential emission spectra of protons and deuterons in reactions induced by ^{3}He at 130 MeV. Breakup data corresponding to two different targets, ^{93}Nb and ^{197}Au, were analyzed. Deuteron differential spectra were compared to the experimental data from [7], while proton emission spectra were presented for completeness. The optical potential of Becchetti-Greenlees was tested, but did not provide a good description of the experimental data due to the incident energy of the experiment. Good agreement to the measurements was obtained
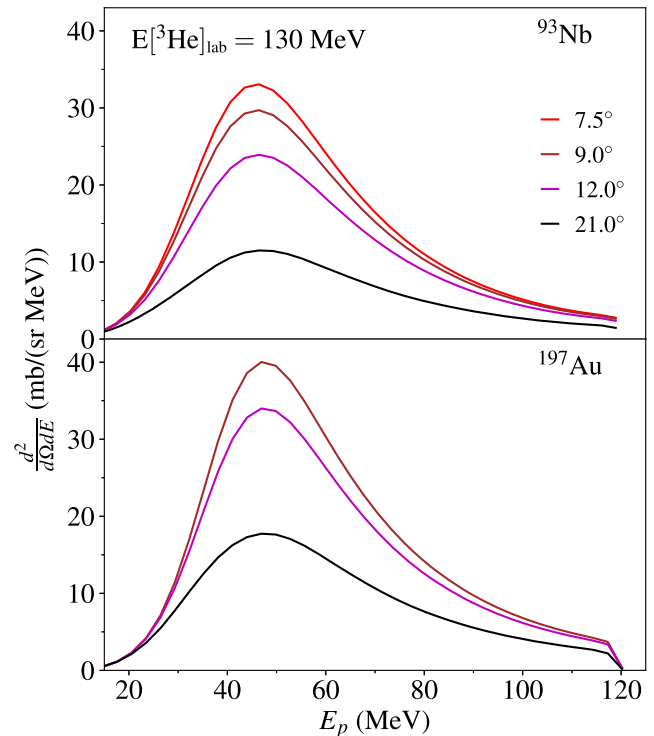
by using the São Paulo potential with a modified value of the nuclear diffuseness. The large value for the diffuseness parameter obtained directly from the SPP leads to a strongly absorptive potential, which furnishes only half of the experimental cross section. We decided to adjust a_0 in order to keep the simple parameterization N_I=0.78. This choice renormalizes the real part of the interaction by about 1% when compared to the original SPP. The choice of a_0 = 0.65 fm follows more closely the values for the diffusivity frequently found in standard optical potentials. This approach facilitates the numerical implementation and provide an easy way of parametrizing the potential for different targets. The zero-range approximation to the DWBA breakup amplitude provided a very good description of the experimental data. The existence of low-energy fragments in the data is understood as being due to compound nucleus emission, a process not included in our model. In general, we have obtained distributions very close in shape and in average values to the reaction measurements. We have thus verified the capability of the model to describe inclusive deuteron emission from ^{3}He-induced reactions.

Although not studied in this work, neutron and diproton (pp) emissions from ^{3}He breakup can also contribute to the reaction dynamics and should be taken into account if one aims to obtain a complete description of the experimental data. We plan to include this emission channel as well, in a forthcoming study. We note that this breakup

channel introduces a new level of complexity, as its correct description requires the inclusion of three-body breakup [27]. Compound nucleus emission should also be taken into account in a complete description of differential fragment spectra, as it makes a significant contribution at backward angles.

In the future, we also plan to extend our calculations to heavier projectiles, where the extra degrees of freedom involved in the system can increase the number and variety of emitted fragments. In these cases, the São Paulo potential can be used to represent the ejectile as well as the projectile-target interaction.

We believe that this study helps advance our understanding of the mechanisms for particle emission in reactions induced by weakly bound nuclei. A complete description and understanding of reactions involving two-fragment projectiles will contribute to the extension of the formalism to three-or-more-fragment reactions.

Compliance with Ethical Standards

Conflict of interests The authors declare that they have no conflict of interest.

References

1. S.M. Qaim, F. Tárkányi, R. Capote, *Nuclear data for the production of therapeutic radionuclides*. Technical Reports Series (International Atomic Energy Agency, Vienna, 2012)
2. G.B. Saha, *Physics and radiobiology of nuclear medicine* (Springer Verlag, New York, 2013)
3. J.E. Escher, J.T. Burke, F.S. Dietrich, N.D. Scielzo, I.J. Thompson, W. Younes, Compound-nuclear reaction cross sections from surrogate measurements. Rev. Mod. Phys. **84**, 353–397 (2012)
4. J. Lei, A.M. Moro, Reexamining closed-form formulae for inclusive breakup: Application to deuteron- and ^{6}Li -induced reactions. Phys. Rev. C **92**, 044616 (2015)
5. A. Di Pietro, A.M. Moro, J. Lei, R. de Diego, Insights into the dynamics of breakup of the halo nucleus 11be on a 64zn target. Physics Letters B **798**, 134954 (2019)
6. N. Matsuoka, A. Shimizu, K. Hosono, T. Saito, M. Kondo, H. Sakaguchi, A. Goto, F. Ohtani, Angular correlation of (3he, pd) reactions at 90 mev and elastic break-up of 3he particles. Nucl. Phys. A **337**(2), 269–284 (1980)
7. A. Djaloeis, J. Bojowald, S. Gopal, W. Oelert, N.G. Puttaswamy, P. Turek, C. Mayer-Böricke, Breakup of ^{3}He projectiles at an incident energy of 43.3 mev/nucleon. Phys. Rev. C **27**, 2389–2392 (1983)
8. E.H.L. Aarts, R.A.R.L. Malfliet, R.J. De Meijer, S.Y. Van der Werf, Reaction mechanisms in ^{3}he projectile breakup at 52 mev on ^{12}c, ^{28}si and ^{58}ni. Nucl. Phys. A **425**, 23–92 (1984)
9. R. Serber, The production of high energy neutrons by stripping. Phys. Rev. **72**, 1008 (1947)
10. N. Austern, C.M. Vincent, Inclusive breakup reactions. Phys. Rev. C **23**, 1847–1853 (1981)
11. T. Udagawa, T. Tamura, Derivation of breakup-fusion cross sections from the optical theorem. Phys. Rev. C **24**, 1348–1349 (1981)
12. A. Kasano, M. Ichimura, A new formalism of inclusive breakup reactions and validity of the surface approximation. Physics Letters B **115**(2), 81–85 (1982)
13. M. Ichimura, N. Austern, C.M. Vincent, Equivalence of post and prior sum rules for inclusive breakup reactions. Phys. Rev. C **32**, 431–439 (1985)
14. M.S. Hussein, K. McVoy, Inclusive projectile fragmentation in the spectator model. Nucl. Phys. A **445**, 124–139 (1985)
15. M. Ichimura, Relation among theories of inclusive breakup reactions. Phys. Rev. C **41**, 834–840 (1990)
16. J. Lei, A.M. Moro, Numerical assessment of post-prior equivalence for inclusive breakup reactions. Phys. Rev. C **92**, 061602(R) (2015)
17. B.V. Carlson, R. Capote, M. Sin, Inclusive proton emission spectra from deuteron breakup reactions. Few-Body Syst **57**, 307–314 (2016)
18. G. Potel, F.M. Nunes, I.J. Thompson, Establishing a theory for deuteron-induced surrogate reactions. Phys. Rev. C **92**, 034611 (2015)
19. G. Potel, G. Perdikakis, B. V. Carlson, Toward a complete theory for predicting inclusive deuteron breakup away from stability. Eur. Phys. J. A **53**, 178 (2017)
20. P.J.A. Buttle, L.J.B. Goldfarb, Finite range effects in deuteron stripping processes. Proc. Phys. Soc. **83**(5), 701–717 (1964)
21. A.J. Koning, J.P. Delaroche, Local and global nucleon optical models from 1 kev to 200 mev. Nucl. Phys. A **713**(3), 231–310 (2003)
22. Y. Han, Y. Shi, Q. Shen, Deuteron global optical model potential for energies up to 200 mev. Phys. Rev. C **74**, 044615 (2006)
23. J.F.D. Becchetti, G.W. Greenlees, Annual Report of J. H. Williams Laboratory, University of Minnesota (1969)
24. L.C. Chamon, B.V. Carlson, L.R. Gasques, D. Pereira, C. De Conti, M.A.G. Alvarez, M.S. Hussein, M.A. Cândido Ribeiro, E.S. Rossi, C.P. Silva, Toward a global description of the nucleus-nucleus interaction. Phys. Rev. C **66**, 014610 (2002)
25. L.C. Chamon, The São Paulo potential. Nucl. Phys. A **787**(1), 198–205 (2007). Proceedings of the Ninth International Conference on Nucleus-Nucleus Collisions
26. I.J. Thompson, F.M. Nunes, *Nuclear reactions for astrophysics: Principles, calculation and applications of low-energy reactions* (Cambridge University Press, Cambridge, 2009)
27. B.V. Carlson, T. Frederico, M.S. Hussein, Inclusive breakup of three-fragment weakly-bound nuclei. Physics Letters B **767**, 53–57 (2017)

Publisher's Note Springer Nature remains neutral with regard to jurisdictional claims in published maps and institutional affiliations.